Interneurons Regulate Locomotion Quiescence via Cyclic Adenosine Monophosphate Signaling During Stress-Induced Sleep in *Caenorhabditis elegans*

Alana Cianciulli, Lauren Yoslov, Kristen Buscemi, Nicole Sullivan, Ryan T. Vance, Francis Janton, Mary R. Szurgot, Thomas Buerkert, Edwin Li, and Matthew D. Nelson[1]
Department of Biology, Saint Joseph's University, Philadelphia, Pennsylvania 19131
ORCID ID: 0000-0002-2085-8974 (M.D.N.)

ABSTRACT Sleep is evolutionarily conserved, thus studying simple invertebrates such as *Caenorhabditis elegans* can provide mechanistic insight into sleep with single cell resolution. A conserved pathway regulating sleep across phylogeny involves cyclic adenosine monophosphate (cAMP), a ubiquitous second messenger that functions in neurons by activating protein kinase A. *C. elegans* sleep in response to cellular stress caused by environmental insults [stress-induced sleep (SIS)], a model for studying sleep during sickness. SIS is controlled by simple neural circuitry, thus allowing for cellular dissection of cAMP signaling during sleep. We employed a red-light activated adenylyl cyclase, IlaC22, to identify cells involved in SIS regulation. We found that pan-neuronal activation of IlaC22 disrupts SIS through mechanisms independent of the cAMP response element binding protein. Activating IlaC22 in the single DVA interneuron, the paired RIF interneurons, and in the CEPsh glia identified these cells as wake-promoting. Using a cAMP biosensor, epac1-camps, we found that cAMP is decreased in the RIF and DVA interneurons by neuropeptidergic signaling from the ALA neuron. Ectopic overexpression of sleep-promoting neuropeptides coded by *flp-13* and *flp-24*, released from the ALA, reduced cAMP in the DVA and RIFs, respectively. Overexpression of the wake-promoting neuropeptides coded by *pdf-1* increased cAMP levels in the RIFs. Using a combination of optogenetic manipulation and *in vivo* imaging of cAMP we have identified wake-promoting neurons downstream of the neuropeptidergic output of the ALA. Our data suggest that sleep- and wake-promoting neuropeptides signal to reduce and heighten cAMP levels during sleep, respectively.

KEYWORDS *Caenorhabditis elegans*; cAMP; optogenetics; sleep

SLEEP is an essential and conserved behavior, which likely exists in some form in all animals (Anafi *et al.* 2019). The molecular regulation of sleep is conserved from invertebrates, such as *Caenorhabditis elegans* and *Drosophila melanogaster*, to mammals. However, the molecules that control sleep/wake cycles in these animals have not been fully described. One pathway that is conserved across phylogeny, which regulates sleep/wake, involves cyclic adenosine monophosphate (cAMP)/Protein Kinase A (PKA) (Crocker and Sehgal 2010). cAMP/PKA pathways are more active during wake and less active during sleep in mice, *D. melanogaster* and *C. elegans* (Hendricks *et al.* 2001; Graves *et al.* 2003; Belfer *et al.* 2013). However, the local cellular dynamics of this pathway and how it is mechanistically linked to behavior is mostly unclear.

cAMP levels are regulated upstream via the activation or inhibition of adenylyl cyclases (ACs) by, respectively, activating or inhibitory G protein–coupled receptors (GPCRs), and downstream via its degradation by phosphodiesterases. A key mediator downstream of cAMP is PKA, whose regulatory subunit binds to cAMP, thus freeing its catalytic subunit to phosphorylate downstream targets (Beebe 1994). Activated PKA has differing effects on its substrates. For example, PKA phosphorylation of the transcription factor cyclic AMP-dependent binding protein (CREB) results in nuclear translocation and activation of gene transcription (Brindle and Montminy 1992), whereas PKA phosphorylation inhibits the metabolic

doi: https://doi.org/10.1534/genetics.119.302293
Manuscript received March 19, 2019; accepted for publication July 8, 2019; published Early Online July 10, 2019.
Supplemental material available at FigShare: https://doi.org/10.25386/genetics.8847728.
[1]Corresponding author: Department of Biology, Saint Joseph's University, 5600 City Ave., Philadelphia, PA 19131. E-mail: mnelson@sju.edu

regulator 5′ AMP-activated protein kinase (Djouder *et al.* 2010).

PKA/CREB plays a central role in regulating sleep and wakefulness; CREB-deficient mice display decreased waking and increased sleep (Graves *et al.* 2003). In both *D. melanogaster* sleep and *C. elegans* developmentally timed sleep (DTS), CREB mutants show reduced wakefulness and increased total sleep (Hendricks *et al.* 2001; Singh *et al.* 2014). *C. elegans* DTS more closely resembles circadian sleep in mammals since it is timed by the *C. elegans* homolog of Period, called LIN-42 (Monsalve *et al.* 2011). Stress-induced sleep (SIS) is a sleep behavior that occurs following cellular damage, which allows for recovery, thus resembles sleep during sickness (Anafi *et al.* 2019). DTS and SIS are regulated by distinct but overlapping mechanisms (Trojanowski *et al.* 2015); a role for cAMP/PKA or CREB during the regulation of SIS has not yet been described. Because of the simple circuitry of SIS (Hill *et al.* 2014), we sought to define such a role and identify cells in which these molecules are functioning during SIS.

Powerful tools have been developed to allow for the optogenetic manipulation of cAMP levels in living cells. Light-activated ACs, including PACα (Weissenberger *et al.* 2011), IlaC22 (Ryu *et al.* 2014), and PaaC (Etzl *et al.* 2018), can increase cAMP following stimulation by specific wavelengths of light. In *C. elegans*, these tools can effectively manipulate simple behaviors such as locomotion; however, they have not been used to study more complex behaviors like sleep. The IlaC22 and PaaC tools have a unique benefit for studying sleep in *C. elegans* because they are activated by light in the near infrared spectrum, a wavelength of light that does not affect behavior (Edwards *et al.* 2008); blue light wakes animals during sleep (Nelson *et al.* 2013). Additionally, tools have been developed to allow for the observation of cAMP dynamics in live cells (Nikolaev *et al.* 2004; Hackley *et al.* 2018). These tools have been used in cell culture (Nikolaev *et al.* 2004; Börner *et al.* 2011) and in dissected *D. melanogaster* brains (Shafer *et al.* 2008; Hackley *et al.* 2018), but not yet in a living, freely behaving animal. While a Förster resonance energy transfer–based cGMP biosensor, cGi500, has been used successfully *in vivo* in *C. elegans* to study sensory behavior (Couto *et al.* 2013; Shidara *et al.* 2017), a cAMP biosensor has not. Thus, we sought to combine optogenetic manipulation and *in vivo* imaging of cAMP during sleep, using *C. elegans* SIS as a model, because of its simple circuitry.

By activating IlaC22 in all neurons, we show that an inhibition of cAMP/PKA signaling is required for locomotion, but not for defecation or feeding quiescence, during SIS. Also, we find that although cAMP/PKA partially signals through CRH-1/CREB to promote wakefulness during DTS, CRH-1 is required for normal levels of SIS, revealing a sleep-promoting role for CRH-1. More selective activation of IlaC22 identified *twk-16*–expressing cells as wake-promoting cells, which includes the RIF and DVA interneurons and the CEPsh glia. Using the epac1-camps biosensor, we show that the RIF and DVA interneurons display lower levels of cAMP during SIS compared to animals lacking a functional ALA neuron that have impaired SIS. Ectopic overexpression of *flp-13* decreases cAMP in the DVA and overexpression of *flp-24* decreases cAMP in the RIFs, while overexpression of *pdf-1* increases cAMP in the RIFs. Thus, we have identified new cells downstream of the ALA that display reduced cAMP signaling during SIS and respond to known sleep/wake regulating neuropeptides.

Materials and Methods

Worm maintenance and strains

Animals were maintained at 20° on agar plates containing nematode growth medium and fed the OP50 derivative bacterial strain DA837 (Davis *et al.* 1995). The following strains were used:

N2 (Bristol).
KG532=*kin-2*(*ce179*).
IB16=*ceh-17*(*np1*).
YT17=*crh-1*(*tz2*).
MT4973=*crh-1*(*n3315*).
NQ570=*qnIs303*[*hsp-16.2p*:*flp-13*;*hsp-16.2p*:*gfp*;*rab-3p*:*mCherry*].
SJU21=*stjEx12*[*twk-16p*:*IlaC22*/SL2/*dsRed*;*myo-2p*:*gfp*].
SJU22=*stjEx13*[*twk-16p*:*IlaC22*/SL2/*dsRed*;*myo-2p*:*gfp*].
SJU26=*stjEx17*[*twk-16p*:*IlaC22*/SL2/*dsRed*;*myo-2p*:*gfp*].
SJU36=*stjEx24*[*snb-1p*:*IlaC22*/SL2/*dsRed*;*myo-2p*:*gfp*].
SJU38=*stjEx26*[*snb-1p*:*IlaC22*/SL2/*dsRed*;*myo-2p*:*gfp*].
SJU39=*stjIs24*[*snb-1p*:*IlaC22*/SL2/*dsRed*;*myo-2p*:*gfp*].
SJU81=*qnIs303*;*stjEx12*.
SJU86=*stjEx70*[*twk-16*(*cs1*)*p*:*IlaC22*/SL2/*dsRed*;*myo-2p*:*gfp*].
SJU87=*stjEx71*[*twk-16*(*cs1*)*p*:*IlaC22*/SL2/*dsRed*;*myo-2p*:*gfp*].
SJU88=*stjEx72*[*twk-16*(*cs1*)*p*:*IlaC22*/SL2/*dsRed*;*myo-2p*:*gfp*].
SJU98=*stjEx78*[*unc-17p*:*epac1-camps*;*unc-17p*:*IlaC22*/SL2/*dsRed*;*myo-2p*:*mCherry*].
SJU129=*stjEx98*[*snb-1p*:*PaaC*;*myo-2p*:*gfp*].
SJU131=*stjEx100*[[*snb-1p*:*PaaC*;*myo-2p*:*gfp*].
SJU134=*crh-1*(*tz2*);*stjIs24*.
SJU167=*stjEx116*[*twk-16p*:*epac1-camps*; *rol-6*(+)].
SJU168=*stjIs116*[*twk-16p*:*epac1-camps*; *rol-6*(+)].
SJU170=*ceh-17*(*np1*);*stjIs116*.
SJU179=*stjEx123*[*pdfr-1p*:*IlaC22*/SL2/*dsRed*;*twk-16p*:*gfp*].
SJU180=*stjEx124*[*pdfr-1p*:*IlaC22*/SL2/*dsRed*;*twk-16p*:*gfp*].
SJU181= *stjEx125*[*pdfr-1p*:*IlaC22*/SL2/*dsRed*;*twk-16p*:*gfp*].
SJU182= *stjEx126*[*hlh-17p*:*IlaC22*/SL2/*dsRed*;*twk-16p*:*gfp*].
SJU183= *stjEx127*[*hlh-17p*:*IlaC22*/SL2/*dsRed*;*twk-16p*:*gfp*].
SJU184= *stjEx128*[*hlh-17p*:*IlaC22*/SL2/dsRed;*twk-16p*:*gfp*].
SJU213= *ceh-17*(*np1*);*stjIs116*;*stjEx149*[*hsp-16.2p*:*flp-13*;*myo-3p*:*mCherry*].
SJU214= *ceh-17*(*np1*);*stjIs116*;*stjEx150*[*hsp-16.2p*:*flp-13*;*myo-3p*:*mCherry*].

SJU215= *ceh-17*(*np1*);*stjIs116*;*stjEx151*[*hsp-16.2p*:*flp-13*;*myo-3p*:*mCherry*].
SJU216= *ceh-17*(*np1*);*stjIs116*;*stjEx152*[*hsp-16.2p*:*pdf-1*;*myo-3p*:*mCherry*].
SJU217= *ceh-17*(*np1*);*stjIs116*;*stjEx153*[*hsp-16.2p*:*pdf-1*;*myo-3p*:*mCherry*].
SJU218= *ceh-17*(*np1*);*stjIs116*;*stjEx154*[*hsp-16.2p*:*pdf-1*;*myo-3p*:*mCherry*].
SJU219= *ceh-17*(*np1*);*stjIs116*;*stjEx155*[*hsp-16.2p*:*flp-24*;*myo-3p*:*mCherry*].
SJU220= *ceh-17*(*np1*);*stjIs116*;*stjEx156*[*hsp-16.2p*:*flp-24*;*myo-3p*:*mCherry*].
SJU221= *ceh-17*(*np1*);*stjIs116*;*stjEx157*[*hsp-16.2p*:*flp-24*;*myo-3p*:*mCherry*].
SJU237= *stjEx163*[*twk-16p*:*kin-2*(RNAi-sense); *twk-16p*:*kin-2*-(RNAi-antisense); *myo-2p*:*mCherry*].
SJU239= *stjEx165*[*twk-16p*:*kin-2*(RNAi-sense); *twk-16p*:*kin-2*(RNAi-antisense); *myo-2p*:*mCherry*].
SJU240= *stjEx166*[*twk-16p*:*kin-2*(RNAi-sense); *twk-16p*:*kin-2*-(RNAi-antisense); *myo-2p*:*mCherry*].

Molecular biology and transgenesis

The DNA constructs expressed in *C. elegans* were made by overlap-extension PCR, as previously described (Nelson and Fitch 2011). Briefly, a promoter was amplified from genomic DNA using PCR. Next, the coding sequence of either IlaC22 or PaaC was amplified from plasmids pSJU1 or pMA-T_PaaC, respectively. Both sequences were codon-adapted for enhanced expression in *C. elegans* (Redemann *et al.* 2011). The operon sequence from the genes *gpd-2/-3* and the dsRed coding sequence were amplified from the plasmid pLR304 (a gift from David Raizen, University of Pennsylvania). The three pieces were fused together by PCR; the oligonucleotides used are listed in the Supplemental Material (Table S1). Microinjection of DNA was performed as described (Stinchcomb *et al.* 1985), the extrachromosomal arrays are listed in Table S2. For the strains SJU86-88, the *twk-16p*(*cs1*):IlaC22:dsRed construct was made by first fusing the *cs1* element to the *pes-10* basal promoter amplified from genomic DNA and the Andy Fire vector L3135 (Addgene), respectively, followed by fusion to IlaC22 and the operon sequence from the genes *gpd-2/-3* and the dsRed coding sequence. To drive expression of *kin-2* double-strand RNA in the *twk-16*–expressing cells, the promoter of *twk-16* was fused to the genomic sequence of *kin-2* spanning the region +4620 to +5594 in the sense orientation. A distinct construct was made where the *twk-16* promoter was fused to a portion of the *kin-2* gene spanning the same nucleotides but in the antisense orientation. Both of these constructs lacked a 3′-UTR, and were injected together into wild-type animals. The *twk-16p*:*epac1-camps* plasmid pSJU6 was constructed by first amplifying the promoter sequence of *twk-16* from genomic DNA, adding a *Nar*I restriction site to the 5′end and a *Kpn*I site to the 3′ end. The amplicon was cut and ligated into the plasmid pSJU4, which contains the codon adapted *epac1-camps* sequence and the *unc-54* 3′-UTR. The *unc-17p*:*epac1-camps* plasmid pSJU2 was created by amplifying the *unc-17* promoter from genomic DNA by PCR, adding a *Bg*III restriction site at the 5′ end and a *Pvu*I site at the 3′ end, and by amplifying the *unc-54* 3′-UTR from genomic DNA, adding a *Xho*I site at the 5′ end and an *Apa*I at the 3′ end. The amplicons were ligated into a Pepac1-camps plasmid (a gift from Ted Abel, University of Iowa). The strains SJU39 and SJU168, derived from SJU36 and SJU167, respectively, were integrated using UV irradiation, as previously described (Mello and Fire 1995).

Locomotion quiescence quantification

Locomotion quiescence during both DTS and SIS was quantified using the WorMotel, as previously described (Churgin *et al.* 2017). Briefly, for DTS, active L4 wild-type, mutant, or transgenic animals were picked individually to 24-welled polydimethylsiloxane (PDMS) microchips (gifts from Chris Fang-Yen, University of Pennsylvania). Images were taken every 10 sec for 12 hr, and quiescence was quantified as described (Churgin *et al.* 2017). For SIS, L4 wild-type, mutant, and/or transgenic animals were picked to freshly seeded plates the day prior to experiments. First-day adult animals were loaded on a 24-welled PDMS chip and exposed to 1500 J/m^2 of UV light using a UV-cross linker (Ultraviolet, 254 UVP) or a 37° water bath for 30 min. One UV-induced SIS experiment (Figure 1B) was performed using a Stratalinker 1800 (Stratagene) at the same energy. Following the stress, images were taken every 10 sec for 4–8 hr and quiescence was measured. During this time, animals were exposed to either four green or red 4.7 inch flexible LED strips (Oznium). For both DTS and SIS, each genotype was averaged over multiple trials and compared to the other genotypes run during the same trials using Student's *t*-test or one-way ANOVA. Wells were censored when an animal was out of view of the camera.

Defecation quiescence quantification

Defecation rate was quantified manually by visual inspection using a dissection microscope. L4 wild-type, mutant, and/or transgenic animals were picked the day prior to the experiment to freshly seeded plates. To quantify defecation rate during SIS, animals were exposed to 1500 J/m^2 of UV light using a UV cross-linker and the number of expulsions were quantified for 5 min between 85 and 95 min postshock. To quantify basal defecation rate, the animals were prepared in the same fashion but not exposed to UV light.

Feeding quiescence quantification

L4 wild-type, mutant, and/or transgenic animals were picked to freshly seeded plates the day prior to the experiment. To quantify feeding quiescence during SIS, animals were exposed to 1500 J/m^2 of UV light using a UV cross-linker and the number of pumps in 20 sec were counted between 85 and 95 min postshock, as previously described (Raizen *et al.* 2012). To quantify basal pumping rate, the animals were prepared in the same fashion but not exposed to UV light.

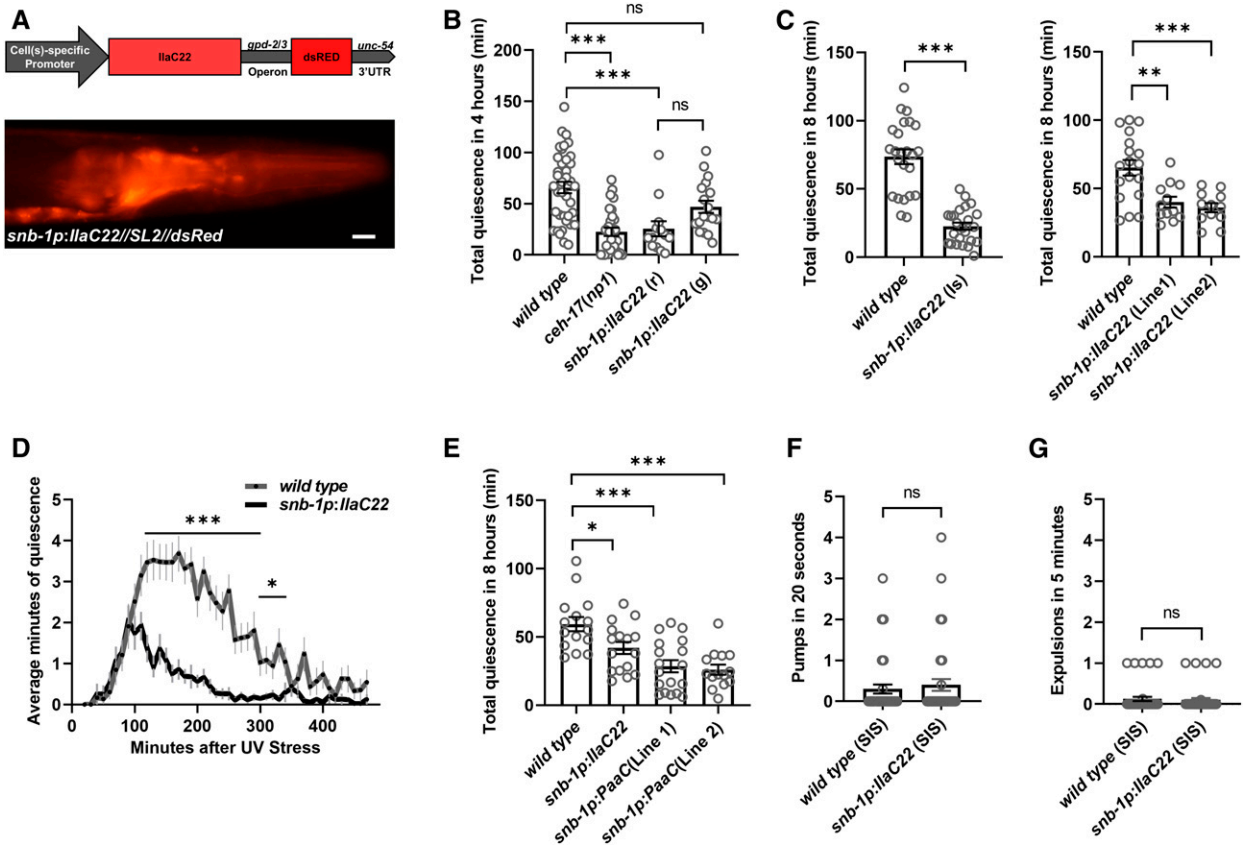

Figure 1 Optogenetic induction of cAMP in the nervous system disrupts sleep. (A) Schematic of the IlaC22-expression constructs used in this study. A tissue/cell-specific promoter was fused to the IlaC22 coding sequence followed by and artificial operon and the coding sequence for dsRed. The image below shows a representative image of the head of a *snb-1p:IlaC22* transgenic animal. Bar, 20 μm. (B) Locomotion quiescence during UV-induced SIS in wild-type, *ceh-1*(*np1*), and *snb-1p:IlaC22* animals under either constant red light (r) or green light (g) for 4 hr ($N \geq 12$, *** $P < 0.001$). Statistical significance was calculated using one-way ANOVA followed by Tukey's multiple comparisons test. (C) Locomotion quiescence during UV-induced SIS in wild-type and *snb-1p:IlaC22* animals in the presence of red light for 8 hr ($N \geq 18$, ** $P < 0.01$, *** $P < 0.001$). One integrated strain (*ls*) and two extrachromosomal strains (line 1 and line 2) were analyzed. Statistical significance was calculated using Student's *t*-test and one-way ANOVA followed by Tukey's multiple comparisons test, respectively. (D) Average quiescence in 10-min windows over 8 hr during UV-induced SIS ($N = 24$, *** $P < 0.001$, * $P < 0.05$). Statistical significance was calculated using two-way ANOVA followed by Sidak's multiple comparisons test. (E) Locomotion quiescence during UV-induced SIS in wild-type, *snb-1p:IlaC22*, and *snb-1p:PaaC* animals in the presence of red light for 8 hr ($N = 15$ (wild type), $N = 17$ [*snb-1p:IlaC22*(*ls*), $N = 18$ (*snb-1p:PaaC*; line 1), $N = 15$ (*snb-1p:PaaC*; line 2), * $P < 0.05$, *** $P < 0.001$]. Statistical significance was calculated using one-way ANOVA followed by Tukey's multiple comparisons test. (F) Pumping rate of wild-type and *snb-1p:IlaC22* animals at 90 min post-UV shock ($N = 20$). Statistical significance was calculated using Student's *t*-test. (G) Defecation rate of wild-type and *snb-1p:IlaC22* animals at 90 min post-UV shock ($N = 20$). Statistical significance was calculated using Student's *t*-test. All error bars represent mean ± SEM.

Fluorescence microscopy

Imaging of expression patterns of the IlaC22- and epac1-camps–expressing strains was conducted on an Olympus AX70 inverted fluorescence microscope. Day 1 adult transgenic animals were mounted on 5% agar pads and immobilized with 25 mM sodium azide. Cell culture and quantitative imaging of epac1-camps–expressing strains was conducted on a Zeiss Axiovert 40 CFL compound fluorescence microscope equipped with a Photometrics DualView image splitter for simultaneous CFP and YFP imaging.

Measuring cAMP dynamics in vivo

To quantify cAMP levels *in vivo*, the following strains were used: SJU98, SJU168, and SJU170. L4 animals were picked to freshly seeded plates the day prior to the experiment. SJU98 was used as a control as it expresses both IlaC22 and epac1-camps in the same cells. First-day adult animals were immobilized using agarose beads and 10% agar, to eliminate the effects of anesthetics, as previously described (Trojanowski *et al.* 2016). Worms were either left in the dark or exposed to red light using a WenTop remote-controlled RGB LED strip, set to the red channel at maximal intensity. Animals were imaged every 5 min on a Zeiss Axiovert 40 CFL compound fluorescence microscope equipped with an X-cite 120Q light source and a Photometrics DualView image splitter for simultaneous CFP and YFP imaging. For the SIS experiments, the SJU168 and SJU170 strains were used. Different populations of first-day adult animals ($N > 20$ at each time point) were imaged prior to stress and 60, 120,

180, and 240 min following exposure to 1500 J/m^2 of UV light. For more frequent imaging, a minimum of 15 animals were imaged every 5 min, between 45 and 75 min following exposure to 1500 J/m^2 of UV light however, in this case the same animal was imaged at each time point during a single trial. For the *flp-13*, *flp-24* , and *pdf-1* overexpression experiments, different populations of animals were imaged prior to and 2 hr after a 30-min 35° heat shock. The heat shock was applied by immersing a parafilmed plate of first-day adults in a 35° water bath. The CFP and YFP intensities were measured using ZEN software (Zeiss), by drawing three boxes localized within the cytoplasm of the desired cell and averaging these values, and the CFP:YFP ratio was calculated.

Cell culture experiments

HEK293 cells were maintained in Eagle's Minimum Essential Medium (EMEM) supplemented with fetal bovine serum and antibiotic/antimycotic and incubated at 37° and 5% CO_2. Cells were seeded on four-well chambered cover-glasses treated with poly-lysine the day before transfection, and transfected overnight with plasmids encoding the epac1-camps biosensor (a gift from Ted Abel, University of Iowa) using Lipofectamine 2000, following the manufacturer's protocol (Invitrogen, Carlsbad, CA). Experiments were carried out in HEPES-buffered saline, and cells were imaged immediately before, and every minute for 6 min following the addition of 25 μM forskolin and 100 μM 1-Methyl-3-Isobutylxanthine (Sigma-Aldrich, St. Louis, MO). Images were taken using a Zeiss Axiovert 40 CFL compound fluorescence microscope equipped with an X-cite 120Q light source and a Photometrics DualView image splitter for simultaneous CFP and YFP imaging. CFP and YFP intensities were measured using ImageJ (Schneider *et al.* 2012).

Data availability

All strains are available upon request. The authors state that all data necessary for confirming the conclusions presented in the article are represented fully within the article. Supplemental material available at FigShare: https://doi.org/10.25386/genetics.8847728.

Results

Pan-neuronal optogenetic induction of cAMP disrupts SIS in C. elegans

Induction of IlaC22 or PaaC in cholinergic motor neurons increases locomotor activity in awake young adults (Ryu *et al.* 2014; Etzl *et al.* 2018). Because cAMP is a conserved wake-promoting second messenger (Crocker and Sehgal 2010), we hypothesized that activation of IlaC22 or PaaC in neurons that are active during times of wakefulness would inhibit sleep. To test this hypothesis, we codon-optimized IlaC22 for *C. elegans* expression (Redemann *et al.* 2011) (GeneScript), and subsequently created multiple extrachromosomal lines and an integrated transgenic strain that express IlaC22 in all 302 neurons, using the promoter from the gene *snb-1* (Nonet *et al.* 1998). The *snb-1* promoter was placed upstream of an artificial operon (Spieth *et al.* 1993), comprising the sequence of IlaC22 and the coding sequence for dsRed as the downstream gene, to verify expression (Figure 1A). As a first test to determine IlaC22 functionality *in vivo*, we quantified locomotion (body bends), feeding (pumps), and defecation (expulsions) in first-day adults following exposure to green or red light. As expected, *snb-1p*:*IlaC22* animals performed more bends than wild-type animals both in the presence of green and red light, but significantly more during red light exposure (Figure S1A). A basal activity of IlaC22 in the absence of red light has been described in the past (Etzl *et al.* 2018). Next, we quantified feeding and defecation under red light and found that *snb-1p*:*IlaC22* animals displayed a slightly higher but significant increase in pumping rate, but there was not a significant difference in their defecation rate (Figure S1, B and C).

To quantify the effects of IlaC22 activation during SIS, first-day adult wild-type, *ceh-17*(*np1*) animals that are SIS defective (Hill *et al.* 2014) because of a nonfunctional ALA neuron (Pujol *et al.* 2000), and *snb-1p*:*IlaC22* animals were exposed to UV irradiation, as previously described (DeBardeleben *et al.* 2017). Locomotion quiescence was measured for 4-hr, under constant red or green light, using a WorMotel (Churgin *et al.* 2017). We found that *snb-1p*:*IlaC22* animals exposed to red or green light displayed less SIS, although the reduction under green light did not reach the level of significance (Figure 1B). Additionally, we monitored the integrated and two extrachromosomal *snb-1p*:*IlaC22* strains for 8-hr following UV exposure and found a significant reduction in total SIS (Figure 1C) and for the majority of the 8-hr time period (Figure 1D). Next, we expressed the red-light activated enzyme PaaC (Etzl *et al.* 2018) in *snb-1*–expressing neurons and again observed a reduction in SIS during constant red light (Figure 1E). Thus, induction of cAMP in the nervous system promotes arousal during SIS. Additionally, we measured total levels of DTS during L4 lethargus and observed a significant reduction in *snb-1p*:*IlaC22* animals compared to wild type (Figure S1D).

When animals undergo SIS they become quiescent with respect to feeding and their defecation cycle (Nath *et al.* 2016). However, *snb-1p*:*IlaC22* animals displayed normal levels of feeding quiescence and a similar number of defecation events 90 min post UV exposure (Figure 1, F and G). Thus, induction of cAMP, using IlaC22, in the nervous system disrupts locomotion but not feeding or defecation quiescence.

Inhibition of PKA is required for SIS

PKA is a likely downstream target of cAMP during DTS since *kin-2*(*ce179*) reduction of function mutants, where PKA is constitutively active (Charlie *et al.* 2006), display significantly less sleep (Belfer *et al.* 2013; Nagy *et al.* 2014b). Whether PKA inhibition is required for SIS had not been specifically tested, although PKA inhibition is not necessary

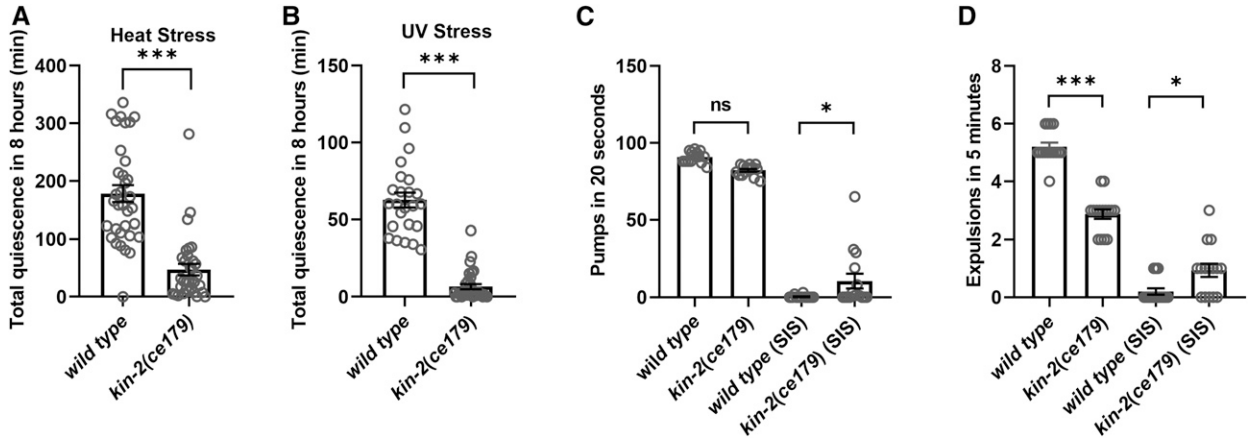

Figure 2 PKA inactivation is required for both heat- and UV-induced SIS. (A) Locomotion quiescence during heat-induced SIS (37° for 30 min) in wild-type and *kin-2*(*ce179*) animals for 8 hr using a WorMotel (N = 32, *** $P < 0.001$). Statistical significance was calculated using Student's *t*-test. (B) Locomotion quiescence during UV-induced SIS in wild-type and *kin-2*(*ce179*) animals for 8 hr using a WorMotel [N = 12 (wild type), N = 30 (*kin-2*), *** $P < 0.001$]. Statistical significance was calculated using Student's *t*-test. (C) Pumping rate before and after UV-induced SIS in wild-type and *kin-2*(*ce179*) animals (N = 15 for each genotype; * $P < 0.05$). Statistical significance was calculated using one-way ANOVA followed by Tukey's multiple comparisons test. (D) Defecation rate of wild-type and *kin-2*(*ce179*) animals pre-UV shock and 90 min post-UV shock (N = 20, *** $P < 0.001$, * $P < 0.05$). Statistical significance was calculated using one-way ANOVA followed by Tukey's multiple comparisons test. All error bars represent mean ± SEM.

for feeding quiescence during heat-induced SIS (Trojanowski *et al.* 2015). To explore the role of PKA in more detail, we measured locomotion, feeding, and defecation quiescence in *kin-2*(*ce179*) mutants during SIS. First, we monitored animals for 8-hr on WorMotels following a 30-min 37° heat shock. We found that locomotion quiescence was significantly decreased in *kin-2*(*ce179*) animals (Figure 2A). The same was observed for UV-induced SIS (Figure 2B). Next, we sought to quantify feeding and defecation quiescence. First, pumping rate prior to stress exposure was not significantly different between *kin-2*(*ce179*) and wild-type animals; however, *kin-2*(*ce179*) displayed impaired feeding quiescence 90 min after UV stress (Figure 2C). *kin-2*(*ce179*) animals displayed a reduced prestress defecation rate (Figure 2D), consistent with the finding that the duration of the defecation motor program is extended in *kin-2* mutants (Nagy *et al.* 2015). Despite this, we observed a suppression of defecation quiescence 90 min after UV stress (Figure 2D). Thus, PKA inhibition is required for quiescence of locomotion, feeding, and defecation during SIS.

CRH-1/CREB does not function downstream of cAMP/PKA during SIS

CREB, coded by *crh-1* in *C. elegans* (Kimura *et al.* 2002), is a downstream target of PKA (Carlezon *et al.* 2005) and promotes arousal in mammals and flies (Hendricks *et al.* 2001; Graves *et al.* 2003). In *C. elegans*, *crh-1* null mutant animals display increased levels of DTS (Singh *et al.* 2014), making CRH-1 the likely target during DTS regulation. We wanted to determine if CRH-1 is functioning downstream of cAMP/PKA during SIS. To do this, we obtained two deletion alleles for *crh-1*, *n3315* and *tz2*. *crh-1*(*tz2*) mutant animals displayed increased DTS (Figure 3A), similar to what was observed with *crh-1*(*n3315*) animals (Singh *et al.* 2014). To determine if CRH-1 is functioning downstream of cAMP/PKA during DTS, we measured locomotion quiescence in *snb-1p*:*IlaC22* and *crh-1*(*tz2*);*snb-1p*:*IlaC22* animals and found that activation of IlaC22 in this context resulted in DTS levels comparable to wild type but not increased to the levels of *crh-1*(*tz2*) animals alone (Figure 3B). Thus, as expected, CRH-1 is a likely downstream target of cAMP/PKA during the regulation of DTS, but PKA likely targets other yet to be identified molecules as well (Figure 3E, DTS model).

Next, we measured locomotion quiescence in both *crh-1*(*tz2*) and *crh-1*(*n3315*) animals during SIS and found that total quiescence was significantly decreased in both strains (Figure 3C). Also, *crh-1*(*tz2*);*snb-1p*:*IlaC22* animals displayed a similar reduction in SIS compared to *crh-1*(*tz2*) animals, which was not additive (Figure 3D). These data suggest that cAMP/PKA signal through yet to be identified downstream factors to promote arousal during SIS and that CREB is activated via PKA-independent mechanisms to promote sleep (Figure 3E, SIS model 1). Alternatively, PKA could inhibit CREB during times of wakefulness (Figure 3E, SIS model 2).

Induction of cAMP in the DVA, RIFs, and CEPsh glial cells disrupts SIS

cAMP levels are regulated by activating and inhibitory GPCRs that modulate AC activity (Beebe 1994). Neuropeptides regulate sleep across phylogeny by signaling through GPCRs (Trojanowski and Raizen 2016); during SIS, the ALA neuron releases neuropeptides that act on unknown target cells to initiate sleep (Nelson *et al.* 2014; Nath *et al.* 2016), which may occur by inhibiting cAMP/PKA. We proposed that cells expressing the gene *twk-16*, including the DVA interneuron (Salkoff *et al.* 2001), were potential downstream targets of ALA signaling, based upon the expression pattern of the

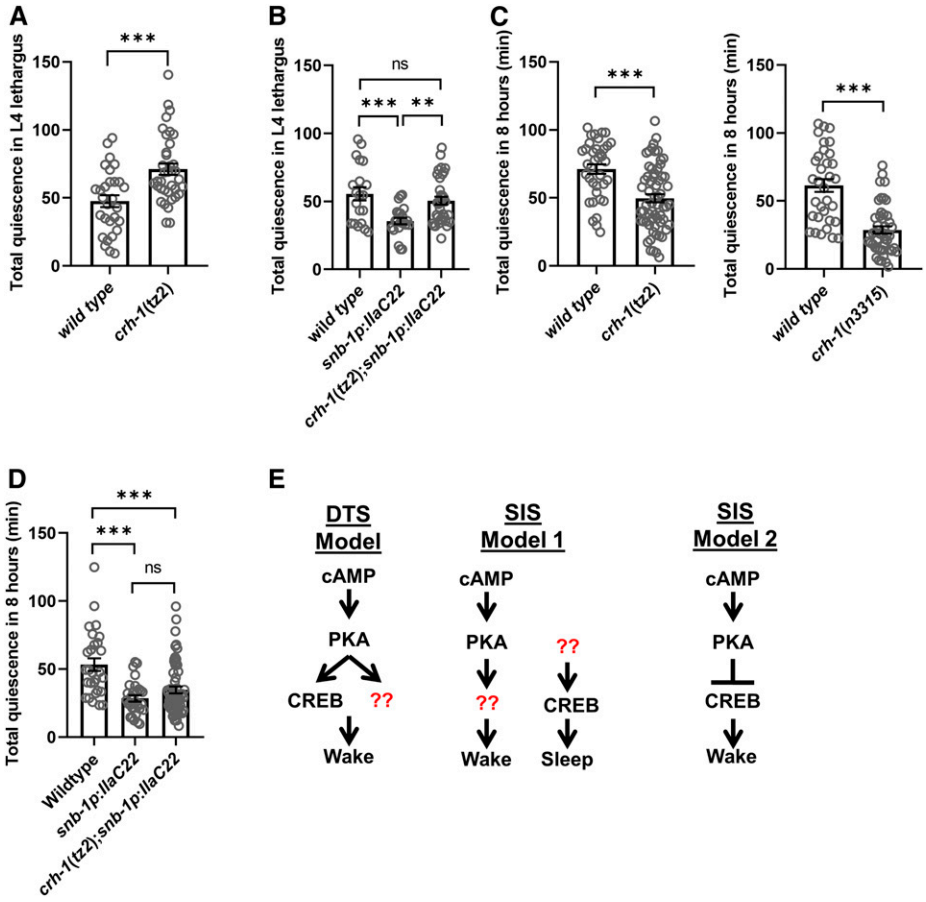

Figure 3 CRH-1/CREB is required for stress-induced sleep. (A) Locomotion quiescence during L4 lethargus in wild-type and *crh-1*(*tz2*) animals ($N = 15$, *** $P < 0.001$). Statistical significance was calculated using Student's *t*-test. (B) Locomotion quiescence during L4 lethargus in wild-type, *snb-1p*:*IlaC22*, and *crh-1*(*tz2*);*snb-1*:*IlaC22* animals ($N > 24$, ** $P < 0.01$, *** $P < 0.001$). Statistical significance was calculated using one-way ANOVA followed by Tukey's multiple comparisons test. (C) Locomotion quiescence during UV-induced SIS in wild-type, *crh-1*(*tz2*), and *crh-1*(*n3315*) animals for 8 hr using a WorMotel ($N > 24$, *** $P < 0.001$). Statistical significance was calculated using one-way ANOVA followed by Tukey's multiple comparisons test. (D) Locomotion quiescence during UV-induced SIS in wild-type, *snb-1p*:*IlaC22*, and *crh-1*(*tz2*);*snb-1*:*IlaC22* animals ($N > 24$, *** $P < 0.001$). Statistical significance was calculated using one-way ANOVA followed by Tukey's multiple comparisons test. (E) Proposed models for cAMP/PKA and CREB signaling during DTS and SIS. All error bars represent mean ± SEM.

sleep-promoting neuropeptide receptor FRPR-4 (Nelson *et al.* 2015). To test this hypothesis, we generated transgenic lines expressing IlaC22 from the *twk-16* promoter. In these lines, we observed intense expression in the DVA and RIF interneurons and the CEPsh glial cells, the latter of which has been implicated in DTS regulation (Katz *et al.* 2018) (Figure S2). We found that *twk-16p*:*IlaC22* animals displayed significantly reduced quiescence compared to wild type (Figure 4A). To determine if these wake-promoting effects were downstream of known SIS regulating pathways, we activated IlaC22 in *twk-16*–expressing cells following overexpression of *flp-13*, a gene that codes for neuropeptides released from the ALA neuron during SIS that are capable of inducing sleep in active adults (Nelson *et al.* 2014; Nath *et al.* 2016). We found that FLP-13–induced quiescence was reduced in *twk-16p*:*IlaC22* animals (Figure S2). Next, to test if PKA is acting in the *twk-16* cells to promote arousal, we generated transgenic RNAi strains that express *kin-2* double-strand RNA in the *twk-16*–expressing cells. We found that SIS was reduced when *kin-2* is knocked down in these cells (Figure 4B). Thus, cAMP/PKA is functioning in the *twk-16*-expressing cells to promote arousal.

Next, we made transgenic animals that express IlaC22 specifically in the DVA interneuron using the enhancer element of the *twk-16* promoter, *cs1* (Puckett Robinson *et al.* 2013) (Figure S2). Activation of IlaC22 in DVA alone reduced SIS in one of three transgenic lines, but not to the same levels seen when activated in all *twk-16*–expressing cells (Figure 4C). Next, we expressed IlaC22 from the promoter of the gene *hlh-17*, which is expressed in the CEPsh glia (McMiller and Johnson 2005) (Figure S2). When IlaC22 was activated in the CEPsh cells, we observed a reduction in SIS in three independent lines, which was less than when activated in all *twk-16*–expressing cells (Figure 4D). Lastly, we expressed IlaC22 in the RIF interneurons using the promoter from the gene *pdfr-1* (Barrios *et al.* 2012) (Figure S2). Activation of IlaC22 in the RIFs also reduced SIS in one of three transgenic lines (Figure 4E). Thus, cAMP induction in the DVA or RIF neurons or the CEPsh glia is sufficient to promote wakefulness during SIS, but not to the same extent when cAMP is induced in all cells together.

cAMP dynamics in the RIF and DVA interneurons are regulated by the ALA neuron

To test the physiological relevance of the cAMP/PKA pathway in the *twk-16*–expressing cells during SIS, we adapted a cAMP biosensor epac1-camps (Nikolaev *et al.* 2004) for use in *C. elegans*. Before expressing epac1-camps *in vivo* we confirmed that we could use this biosensor in cell culture. We transfected HEK293 cells with epac1-camps and treated cells with 25 μM forskolin and 100 μM IBMX and observed a significant increase in cAMP (Figure S4A). To confirm that

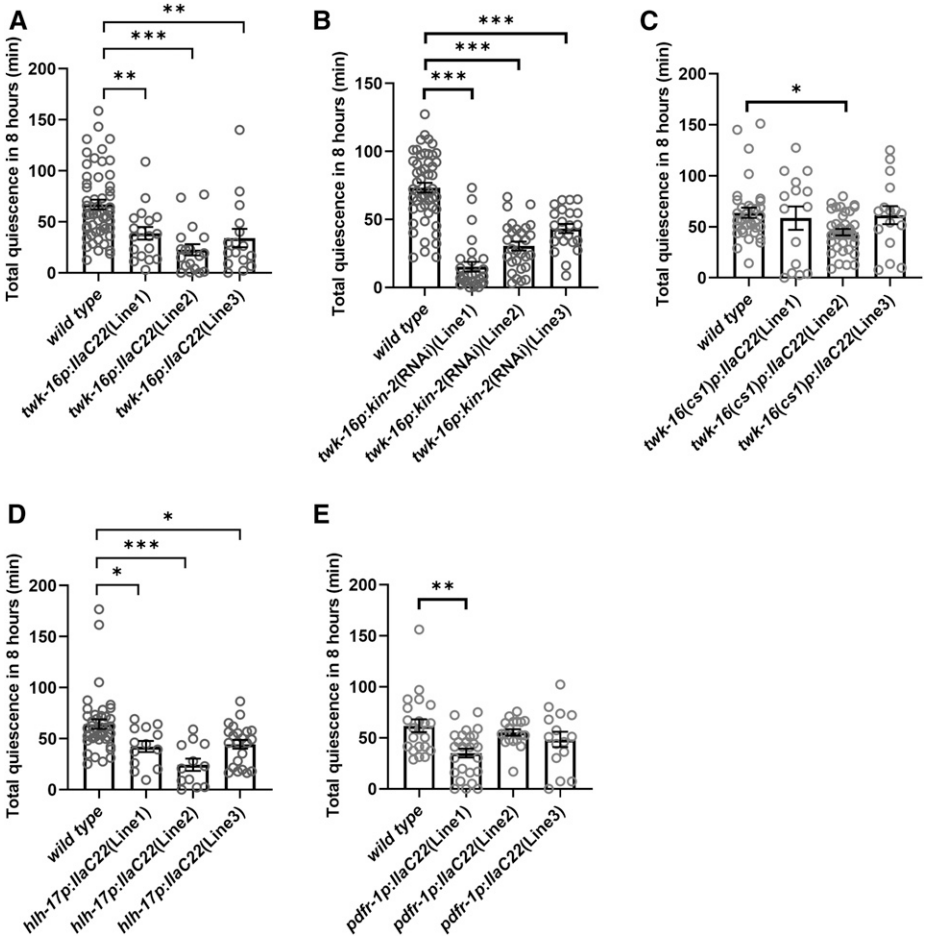

Figure 4 Induction of cAMP in *twk-16*–expressing cells disrupts stress-induced sleep. (A) Locomotion quiescence during UV-induced SIS in wild-type (N = 53) and *twk-16p:IlaC22* animals for 8 hr using a WorMotel (** $P < 0.01$, *** $P < 0.001$). Three extrachromosomal lines were analyzed ($N > 15$ for each line). (B) Locomotion quiescence during UV-induced SIS in wild-type (N = 51) and *twk-16p:kin-2*(RNAi) animals for 8 hr using a WorMotel (*** $P < 0.001$). Three extrachromosomal lines were analyzed ($N > 21$ for each line). (C) Locomotion quiescence during UV-induced SIS in wild-type (N = 35) and *twk-16*(*cs1*)*p:IlaC22* animals for 8 hr using a WorMotel (* $P < 0.05$). Three extrachromosomal lines were analyzed ($N \geq 15$ for each line). (D) Locomotion quiescence during UV-induced SIS in wild-type (N = 40) and *hlh-17p:IlaC22* animals for 8 hr using a WorMotel (* $P < 0.05$, *** $P < 0.001$). Three extrachromosomal lines were analyzed ($N \geq 12$ for each line). (E) Locomotion quiescence during UV-induced SIS in wild-type (N = 22) and *pdfr-1p:IlaC22* animals for 8 hr using a WorMotel (** $P < 0.01$). Three extrachromosomal lines were analyzed ($N \geq 15$ for each line). In each case, statistical significance was calculated using one-way ANOVA followed by Tukey's multiple comparisons test. All error bars represent mean ± SEM.

epac1-camps is functional *in vivo* we made a transgenic line expressing epac1-camps and IlaC22 in cholinergic motor neurons. We exposed these animals to either red light or darkness for 20 min and quantified the CFP:YFP ratio every 5 min. We imaged a single neuron of the paired AIYs and found that cAMP levels increased consistently over the 20-min period (Figure S4B). This suggests that epac1-camps responds to changes in cAMP and that IlaC22 produces measurable increases of cAMP *in vivo* in *C. elegans*.

Next, we codon-adapted epac1-camps for optimal expression in *C. elegans* (Redemann *et al.* 2011) and made an integrated transgenic line expressing epac1-camps from the *twk-16* promoter (Figure S5A). We crossed the integrated *twk-16p:epac1-camps* array into the *ceh-17*(*np1*) mutant background; SIS was quantified to confirm that this strain displayed reduced levels of sleep during SIS (Figure S5B). As a first test, we quantified the CFP:YFP ratio in the DVA, RIF, and CEPsh in different populations of animals before SIS ($T = 0$) and every 60 min for 4-hr following the induction of SIS by UV irradiation. We found that the CFP:YFP ratio was unchanged following UV stress in the DVA and CEPsh glial cells in both the wild-type and *ceh-17*(*np1*) mutant background compared to prestress conditions. However, when we measured the CFP:YFP ratio in the RIF neurons we found that although cAMP levels were not different at 0 and 240 min post-UV shock, cAMP levels were significantly lower in wild-type populations compared to *ceh-17*(*np1*) animals at 60 and 180 min post-UV (Figure 5, A–C). These data suggest that cAMP levels are reduced at detectable levels in the RIFs during SIS in an ALA-dependent manner.

Next, we made more frequent measurements during the peak of UV-induced SIS, between 45 and 75 min post-UV shock in the same animal, and repeated this over multiple trials in both the wild-type and *ceh-17*(*np1*) background. In this context, we found that cAMP levels were significantly lower in wild-type animals at each time point compared to the sleep-defective *ceh-17*(*np1*) mutant animals in both the DVA and RIF interneurons, but not the CEPsh glial cells (Figure 5, D–F). Based on these observations, we propose that earlier and more frequent imaging at the peak of SIS revealed a difference in the DVA between these two strains (Figure 5D). Thus, we also propose that cAMP levels are reduced in the RIFs compared to prestress conditions during SIS in an ALA-dependent manner, and that cAMP levels in the DVA are kept at a basal level by the ALA, but not necessarily reduced below times of wake. These data suggest that cAMP levels are affected in unique ways by neuropeptide signaling in distinct cell types.

FLP-13, FLP-24, and PDF-1 neuropeptides are capable of reducing cAMP in the DVA and RIF interneurons

The ALA neuron releases a collection of sleep-promoting neuropeptides during SIS, including those coded by *flp-13*

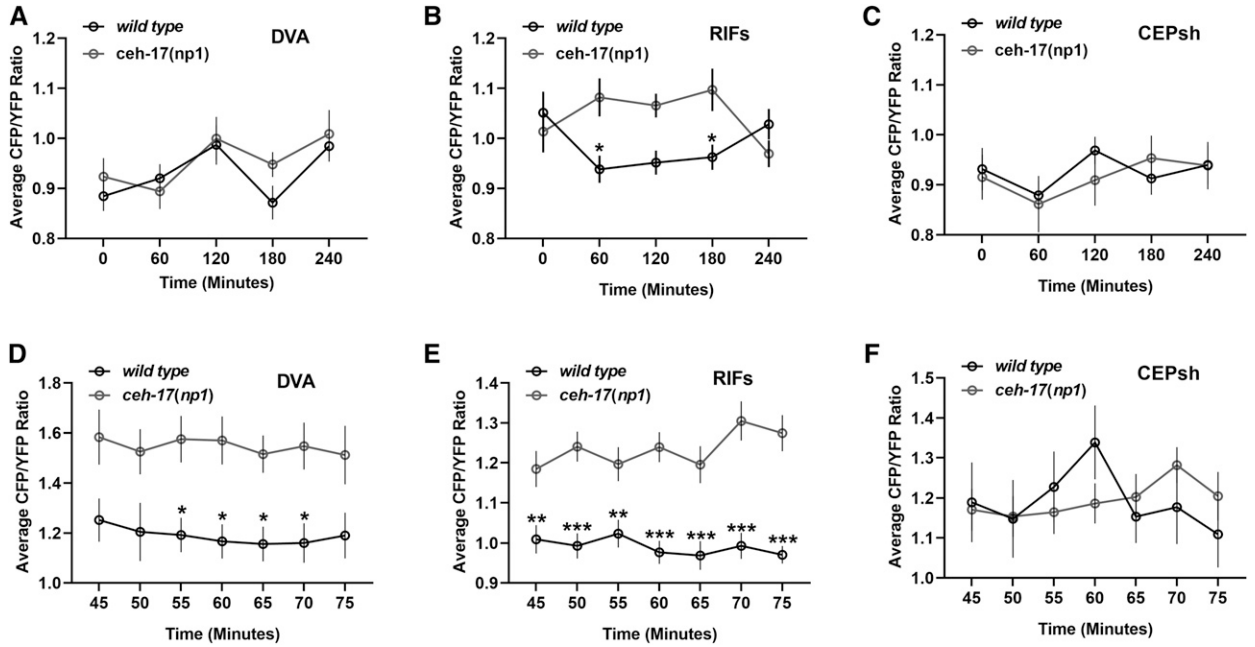

Figure 5 cAMP levels are reduced in the DVA and RIF neurons compared to *ceh-17* mutant animals. (A) Average CFP:YFP ratio in the DVA cell body during UV-induced SIS in wild-type and *ceh-17*(*np1*) animals ($N > 27$ for each time point). (B) Average CFP:YFP ratio in the RIF interneurons during UV-induced SIS in wild-type and *ceh-17*(*np1*) animals ($N > 28$ for each time point; * $P < 0.05$). (C) Average CFP:YFP ratio in the CEPshVL glial cell during UV-induced SIS in wild-type and *ceh-17*(*np1*) animals ($N > 28$ for each time point). For A–C, different populations of animals were imaged at each time point and statistical significance was calculated using one-way ANOVA followed by Tukey's multiple comparisons test. (D) Average CFP:YFP ratio in the DVA from 45 to 75 min post-UV shock SIS in wild-type and *ceh-17*(*np1*) animals ($N = 15$ for each genotype; * $P < 0.05$). (E) Average CFP:YFP ratio in the RIFs from 45 to 75 min post-UV shock in wild-type and *ceh-17*(*np1*) animals ($N = 20$ for each time point; ** $P < 0.01$, *** $P < 0.001$). (F) Average CFP:YFP ratio in the CEPshVL glial cell from 45 to 75 min post-UV shock SIS in wild-type and *ceh-17*(*np1*) animals ($N = 15$ for each genotype). For D–F, the same animal was imaged at each time point and this was repeated over multiple trials. Statistical significance was calculated using two-way ANOVA followed by Sidak's multiple comparisons test. All error bars represent mean ± SEM.

(Nelson *et al.* 2014) and *flp-24* (Nath *et al.* 2016). We predicted that overexpression of sleep-promoting neuropeptides would reduce cAMP in the DVA and/or RIF neurons. To test this, we used an inducible heat-shock promoter from the gene *hsp-16.2* to ectopically overexpress either *flp-13* or *flp-24* in *ceh-17*(*np1*);*twk-16p*:*epac1-camps* animals. We measured the CFP:YFP ratio prior to induction of the *hsp-16.2* promoter, and 2-hr after a 30-min 35° heat shock. Interestingly, we found that *flp-13* overexpression significantly decreased cAMP in the DVA, but not the RIFs or CEPsh cells, whereas *flp-24* overexpression reduced cAMP in the RIFs, but not the DVA or CEPsh cells (Figure 6, A–C). These data suggest that FLP-13 neuropeptides signal to the DVA and FLP-24 neuropeptides signal to the RIFs to promote locomotion quiescence during SIS.

Since the RIFs express the PDFR-1 receptor (Barrios *et al.* 2012) and pigment dispersing factor (PDF) neuropeptides promote arousal in *D. melanogaster* (Renn *et al.* 1999) and *C. elegans* (Choi *et al.* 2013), we hypothesized that overexpression of *pdf-1* would increase cAMP in the RIFs. To test this, we overexpressed the *pdf-1* gene from the *hsp-16.2* promoter in *ceh-17*(*np1*);*twk-16p*:*epac1-camps* animals. Overexpression of *pdf-1* resulted in a significant increase in cAMP in the RIFs, but not in the DVA or CEPsh cells (Figure 6, A–C), suggesting the PDF-1 and FLP-24 neuropeptides play antagonistic signaling roles to the RIFs during the regulation of quiescence during SIS. These data support a model where neuropeptides released by the ALA reduce cAMP in select cells to induce different aspects of sleep, and may reflect a broader role for neuropeptide signaling during sleep regulation in other animals.

Discussion

Neuropeptides regulate complex behaviors like sleep in all animals, yet how behavior is altered by these signaling molecules at the mechanistic level is poorly understood. One common mechanism of neuropeptide signaling may involve the reduction of cAMP/PKA signaling in select neural populations to initiate the various behaviors associated with sleep. We leveraged the simple SIS model of *C. elegans* to test this hypothesis and identify new cells downstream of known neuropeptide circuitry. Specifically, we used the red-light activated AC IlaC22 and an *in vivo* cAMP biosensor, epac1-camps, to identify new cells responsible for regulating SIS in *C. elegans*. Using IlaC22, we showed that pan-neuronal induction of cAMP significantly reduces quiescence during both SIS and DTS. We also showed that this induction of cAMP partially acts through CRH-1/CREB during DTS, but not during SIS, suggesting that the PKA substrates for SIS are

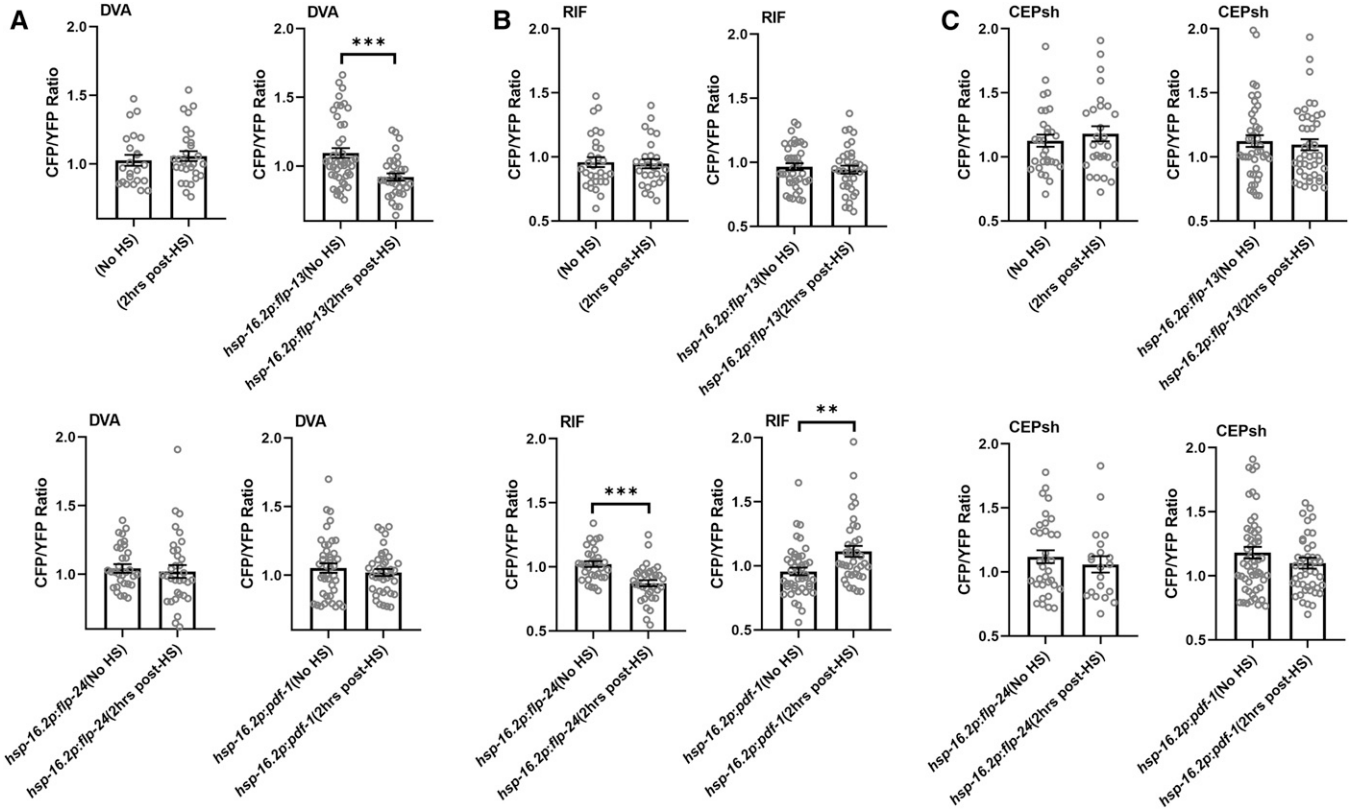

Figure 6 cAMP levels are altered in the RIF and DVA interneurons following neuropeptide overexpression. Average CFP:YFP ratio in the DVA (A), RIF (B), or CEPsh (C) cells pre- and 2 hr post-heat shock in *ceh-17*(*np1*) (controls), *ceh-17*(*np1*);*hsp-16.2p*:*flp-13*, *ceh-17*(*np1*);*hsp-16.2p*:*flp-24*, and *ceh-17*(*np1*);*hsp-16.2p*:*pdf-1* animals ($N > 30$, ** $P < 0.01$, *** $P < 0.001$). Statistical significance was calculated using Student's *t*-test. All error bars represent mean ± SEM.

unique from those of DTS. We then coupled IlaC22 with the cAMP biosensor epac1-camps to show that *twk-16*-expressing cells, including the DVA and RIF interneurons, and CEPsh glial cells are capable of promoting wakefulness, while the RIF and DVA interneurons display a measurable difference in cAMP levels compared to animals that lack a functioning ALA neuron. Moreover, we have shown that sleep-promoting FLP-13 and FLP-24 neuropeptides are capable of reducing cAMP levels in the DVA and RIF interneurons, respectively. We have also shown that overexpression of PDF-1 neuropeptides causes a significant increase in cAMP in the RIFs. These results suggest that both the RIFs and DVA are downstream targets of the neuropeptidergic ALA neuron but are signaled to by distinct neurotransmitters. Overall, our data support a model in which neuropeptides reduce cAMP/PKA in specific neurons to induce the quiescent programs associated with sleep.

The entire *C. elegans* circuitry has been mapped (White *et al.* 1986) which indicates that the DVA and RIFs are highly connected cholinergic interneurons (Pereira *et al.* 2015) that are likely excitatory. We speculate that these neurons are active during times of activity, stimulating locomotion and other aspects of movement that occur during times of wakefulness. The DVA has been shown to function as a stretch mechanoreceptor during locomotion, since abnormal activity of the DVA results in an exaggerated bend posture (Li *et al.* 2006). Additionally, overexpression of the GPCR FRPR-4 in the DVA results in the identical phenotype. Interestingly, deletion of the *flp-13* gene completely suppresses the bend phenotype, suggesting a direct link between the ALA and the DVA (Nelson *et al.* 2015). Our work strengthens that connection and suggests that the DVA likely plays an active role during normal locomotion, which is inhibited by FLP-13 neuropeptides during SIS. Moreover, our data suggest that FLP-13 neuropeptides initiate quiescence of locomotion by inhibiting cAMP/PKA in the DVA. We speculate that this may also be the case when they signal through another known FLP-13 receptor DMSR-1, in other cells (Iannacone *et al.* 2017). By reducing cAMP levels, wake-promoting neurotransmitter release could potentially be inhibited.

The RIF interneurons likely play a role during the regulation of wake activities as well. For example, it has been proposed that the RIFs are inhibited during periods of dwelling and activated during roaming states (Flavell *et al.* 2013). Moreover, PDFR-1 is expressed on the RIF interneurons (Barrios *et al.* 2012), and the PDF-1 signaling pathway promotes both activity during sleep (Choi *et al.* 2013) and a reduction in arousal threshold (Nagy *et al.* 2014a). We hypothesize that both the DVA and RIFs are active during locomotion (*i.e.*, wake) and inhibited during sleep. Our data

suggest that this is accomplished by the ALA neuron where FLP-13 neuropeptides signal to the DVA and FLP-24 neuropeptides to the RIFs, the latter functioning antagonistically with PDF-1 neuropeptides.

An antagonistic balance of cAMP/PKA signaling between somnogenic (*i.e.*, sleep-promoting) neuropeptides and wake-promoting factors might underly sleep regulation in many animals. In *D. melanogaster*, PDF signals to target tissues to increase cAMP to promote wakefulness and stabilize the circadian clock (Shafer *et al.* 2008; Li *et al.* 2014), suggesting that somnogenic factors function to reduce cAMP in the same cells. On the other hand, the vertebrate wake promoting neuropeptide Orexin-B may function by decreasing cAMP in target tissues when signaling specifically to the orexin receptor type-2 (Zhu *et al.* 2003). We speculate that in this context, sleep-promoting molecules may increase cAMP to counterbalance the effects of Orexin signaling. There is also evidence that melatonin, a vertebrate sleep-promoting neuropeptide, may elicit its effects by signaling through the melatonin MT1 receptor and increasing intracellular cAMP. This increase in cAMP may lead to the modulation of ion channel function (Chen *et al.* 2014; Huete-Toral *et al.* 2015), suggesting that wake promoting factors decrease cAMP in these cells. So, although our work suggests that somnogenic neuropeptides largely reduce cAMP levels, work in other animals show that cAMP function is context-dependent and can have different effects based on cell type. A better understanding of the cellular basis of neuropeptide signaling and the effects of cAMP/PKA activation or inhibition in specific cell types will allow for a clearer picture of how sleep behaviors are regulated at the cellular and molecular level.

Acknowledgments

We thank David Raizen, Chris Fang-Yen, and Matt Churgin at the University of Pennsylvania for valuable technical support and David Raizen for comments on our manuscript. We thank Ted Abel, Andreas Winkler, and Anne Hart for sharing plasmids and strains. Some strains were provided by the CGC, which is funded by the National Institutes of Health Office of Research Infrastructure Programs (grant P40 OD010440). We thank the Saint Joseph's University Summer Scholars Program, the John P. McNulty Fellows Program, and the Peter and Dorothy Kowey fellowship for student funding. Research was primarily supported by the National Institute of General Medical Sciences of the National Institutes of Health grant R15GM122058 (Principal Investigator M.D.N.).

Literature Cited

Anafi, R. C., M. S. Kayser, and D. M. Raizen, 2019 Exploring phylogeny to find the function of sleep. Nat. Rev. Neurosci. 20: 109–116. https://doi.org/10.1038/s41583-018-0098-9

Barrios, A., R. Ghosh, C. Fang, S. W. Emmons, and M. M. Barr, 2012 PDF-1 neuropeptide signaling modulates a neural circuit for mate-searching behavior in C. elegans. Nat. Neurosci. 15: 1675–1682. https://doi.org/10.1038/nn.3253

Beebe, S. J., 1994 The cAMP-dependent protein kinases and cAMP signal transduction. Semin. Cancer Biol. 5: 285–294.

Belfer, S. J., H. S. Chuang, B. L. Freedman, J. Yuan, M. Norton *et al.*, 2013 Caenorhabditis-in-drop array for monitoring C. elegans quiescent behavior. Sleep (Basel) 36: 689–698G. https://doi.org/10.5665/sleep.2628

Börner, S., F. Schwede, A. Schlipp, F. Berisha, D. Calebiro *et al.*, 2011 FRET measurements of intracellular cAMP concentrations and cAMP analog permeability in intact cells. Nat. Protoc. 6: 427–438. https://doi.org/10.1038/nprot.2010.198

Brindle, P. K., and M. R. Montminy, 1992 The CREB family of transcription activators. Curr. Opin. Genet. Dev. 2: 199–204. https://doi.org/10.1016/S0959-437X(05)80274-6

Carlezon, Jr., W. A., R. S. Duman, and E. J. Nestler, 2005 The many faces of CREB. Trends Neurosci. 28: 436–445. https://doi.org/10.1016/j.tins.2005.06.005

Charlie, N. K., A. M. Thomure, M. A. Schade, and K. G. Miller, 2006 The Dunce cAMP phosphodiesterase PDE-4 negatively regulates G alpha(s)-dependent and G alpha(s)-independent cAMP pools in the Caenorhabditis elegans synaptic signaling network. Genetics 173: 111–130. https://doi.org/10.1534/genetics.105.054007

Chen, L., X. He, Y. Zhang, X. Chen, X. Lai *et al.*, 2014 Melatonin receptor type 1 signals to extracellular signal-regulated kinase 1 and 2 via Gi and Gs dually coupled pathways in HEK-293 cells. Biochemistry 53: 2827–2839. https://doi.org/10.1021/bi500092e

Choi, S., M. Chatzigeorgiou, K. P. Taylor, W. R. Schafer, and J. M. Kaplan, 2013 Analysis of NPR-1 reveals a circuit mechanism for behavioral quiescence in C. elegans. Neuron 78: 869–880. https://doi.org/10.1016/j.neuron.2013.04.002

Churgin, M. A., S. K. Jung, C. C. Yu, X. Chen, D. M. Raizen *et al.*, 2017 Longitudinal imaging of Caenorhabditis elegans in a microfabricated device reveals variation in behavioral decline during aging. eLife 6: e26652.

Couto, A., S. Oda, V. O. Nikolaev, Z. Soltesz, and M. de Bono, 2013 In vivo genetic dissection of O2-evoked cGMP dynamics in a Caenorhabditis elegans gas sensor. Proc. Natl. Acad. Sci. USA 110: E3301–E3310. https://doi.org/10.1073/pnas.1217428110

Crocker, A., and A. Sehgal, 2010 Genetic analysis of sleep. Genes Dev. 24: 1220–1235. https://doi.org/10.1101/gad.1913110

Davis, M. W., D. Somerville, R. Y. Lee, S. Lockery, L. Avery *et al.*, 1995 Mutations in the Caenorhabditis elegans Na,K-ATPase alpha-subunit gene, eat-6, disrupt excitable cell function. J. Neurosci. 15: 8408–8418. https://doi.org/10.1523/JNEUROSCI.15-12-08408.1995

DeBardeleben, H. K., L. E. Lopes, M. P. Nessel, and D. M. Raizen, 2017 Stress-induced sleep after exposure to ultraviolet light is promoted by p53 in Caenorhabditis elegans. Genetics 207: 571–582.

Djouder, N., R. D. Tuerk, M. Suter, P. Salvioni, R. F. Thali *et al.*, 2010 PKA phosphorylates and inactivates AMPKalpha to promote efficient lipolysis. EMBO J. 29: 469–481. https://doi.org/10.1038/emboj.2009.339

Edwards, S. L., N. K. Charlie, M. C. Milfort, B. S. Brown, C. N. Gravlin *et al.*, 2008 A novel molecular solution for ultraviolet light detection in Caenorhabditis elegans. PLoS Biol. 6: e198. https://doi.org/10.1371/journal.pbio.0060198

Etzl, S., R. Lindner, M. D. Nelson, and A. Winkler, 2018 Structure-guided design and functional characterization of an artificial red light-regulated guanylate/adenylate cyclase for optogenetic applications. J. Biol. Chem. 293: 9078–9089. https://doi.org/10.1074/jbc.RA118.003069

Flavell, S. W., N. Pokala, E. Z. Macosko, D. R. Albrecht, J. Larsch *et al.*, 2013 Serotonin and the neuropeptide PDF initiate and extend opposing behavioral states in C. elegans. Cell 154: 1023–1035. https://doi.org/10.1016/j.cell.2013.08.001

Graves, L. A., K. Hellman, S. Veasey, J. A. Blendy, A. I. Pack *et al.*, 2003 Genetic evidence for a role of CREB in sustained cortical

arousal. J. Neurophysiol. 90: 1152–1159. https://doi.org/10.1152/jn.00882.2002

Hackley, C. R., E. O. Mazzoni, and J. Blau, 2018 cAMPr: a single-wavelength fluorescent sensor for cyclic AMP. Sci. Signal. 11: eaah3738.

Hendricks, J. C., J. A. Williams, K. Panckeri, D. Kirk, M. Tello *et al.*, 2001 A non-circadian role for cAMP signaling and CREB activity in Drosophila rest homeostasis. Nat. Neurosci. 4: 1108–1115. https://doi.org/10.1038/nn743

Hill, A. J., R. Mansfield, J. M. Lopez, D. M. Raizen, and C. Van Buskirk, 2014 Cellular stress induces a protective sleep-like state in C. elegans. Curr. Biol. 24: 2399–2405. https://doi.org/10.1016/j.cub.2014.08.040

Huete-Toral, F., A. Crooke, A. Martinez-Aguila, and J. Pintor, 2015 Melatonin receptors trigger cAMP production and inhibit chloride movements in nonpigmented ciliary epithelial cells. J. Pharmacol. Exp. Ther. 352: 119–128. https://doi.org/10.1124/jpet.114.218263

Iannacone, M. J., I. Beets, L. E. Lopes, M. A. Churgin, C. Fang-Yen *et al.*, 2017 The RFamide receptor DMSR-1 regulates stress-induced sleep in C. elegans. eLife 6: e19837.

Katz, M., F. Corson, S. Iwanir, D. Biron, and S. Shaham, 2018 Glia modulate a neuronal circuit for locomotion suppression during sleep in C. elegans. Cell Rep. 22: 2575–2583. https://doi.org/10.1016/j.celrep.2018.02.036

Kimura, Y., E. E. Corcoran, K. Eto, K. Gengyo-Ando, M. A. Muramatsu *et al.*, 2002 A CaMK cascade activates CRE-mediated transcription in neurons of Caenorhabditis elegans. EMBO Rep. 3: 962–966. https://doi.org/10.1093/embo-reports/kvf191

Li, W., Z. Feng, P. W. Sternberg, and X. Z. Xu, 2006 A C. elegans stretch receptor neuron revealed by a mechanosensitive TRP channel homologue. Nature 440: 684–687. https://doi.org/10.1038/nature04538

Li, Y., F. Guo, J. Shen, and M. Rosbash, 2014 PDF and cAMP enhance PER stability in Drosophila clock neurons. Proc. Natl. Acad. Sci. USA 111: E1284–E1290 (erratum: Proc. Natl. Acad. Sci. USA 111: 8311). https://doi.org/10.1073/pnas.1402562111

McMiller, T. L., and C. M. Johnson, 2005 Molecular characterization of HLH-17, a C. elegans bHLH protein required for normal larval development. Gene 356: 1–10. https://doi.org/10.1016/j.gene.2005.05.003

Mello, C., and A. Fire, 1995 DNA transformation. Methods Cell Biol. 48: 451–482. https://doi.org/10.1016/S0091-679X(08)61399-0

Monsalve, G. C., C. Van Buskirk, and A. R. Frand, 2011 LIN-42/PERIOD controls cyclical and developmental progression of C. elegans molts. Curr. Biol. 21: 2033–2045. https://doi.org/10.1016/j.cub.2011.10.054

Nagy, S., D. M. Raizen, and D. Biron, 2014a Measurements of behavioral quiescence in Caenorhabditis elegans. Methods 68: 500–507. https://doi.org/10.1016/j.ymeth.2014.03.009

Nagy, S., N. Tramm, J. Sanders, S. Iwanir, I. A. Shirley *et al.*, 2014b Homeostasis in C. elegans sleep is characterized by two behaviorally and genetically distinct mechanisms. eLife 3: e04380. https://doi.org/10.7554/eLife.04380

Nagy, S., Y. C. Huang, M. J. Alkema, and D. Biron, 2015 Caenorhabditis elegans exhibit a coupling between the defecation motor program and directed locomotion. Sci. Rep. 5: 17174. https://doi.org/10.1038/srep17174

Nath, R. D., E. S. Chow, H. Wang, E. M. Schwarz, and P. W. Sternberg, 2016 C. elegans stress-induced sleep emerges from the collective action of multiple neuropeptides. Curr. Biol. 26: 2446–2455. https://doi.org/10.1016/j.cub.2016.07.048

Nelson, M. D., and D. H. Fitch, 2011 Overlap extension PCR: an efficient method for transgene construction. Methods Mol. Biol. 772: 459–470. https://doi.org/10.1007/978-1-61779-228-1_27

Nelson, M. D., N. F. Trojanowski, J. B. George-Raizen, C. J. Smith, C. C. Yu *et al.*, 2013 The neuropeptide NLP-22 regulates a sleep-like state in Caenorhabditis elegans. Nat. Commun. 4: 2846. https://doi.org/10.1038/ncomms3846

Nelson, M. D., K. H. Lee, M. A. Churgin, A. J. Hill, C. Van Buskirk *et al.*, 2014 FMRFamide-like FLP-13 neuropeptides promote quiescence following heat stress in Caenorhabditis elegans. Curr. Biol. 24: 2406–2410. https://doi.org/10.1016/j.cub.2014.08.037

Nelson, M. D., T. Janssen, N. York, K. H. Lee, L. Schoofs *et al.*, 2015 FRPR-4 is a G-protein coupled neuropeptide receptor that regulates behavioral quiescence and posture in Caenorhabditis elegans. PLoS One 10: e0142938. https://doi.org/10.1371/journal.pone.0142938

Nikolaev, V. O., M. Bunemann, L. Hein, A. Hannawacker, and M. J. Lohse, 2004 Novel single chain cAMP sensors for receptor-induced signal propagation. J. Biol. Chem. 279: 37215–37218. https://doi.org/10.1074/jbc.C400302200

Nonet, M. L., O. Saifee, H. Zhao, J. B. Rand, and L. Wei, 1998 Synaptic transmission deficits in Caenorhabditis elegans synaptobrevin mutants. J. Neurosci. 18: 70–80. https://doi.org/10.1523/JNEUROSCI.18-01-00070.1998

Pereira, L., P. Kratsios, E. Serrano-Saiz, H. Sheftel, A. E. Mayo *et al.*, 2015 A cellular and regulatory map of the cholinergic nervous system of C. elegans. eLife 4: e12432.

Puckett Robinson, C., E. M. Schwarz, and P. W. Sternberg, 2013 Identification of DVA interneuron regulatory sequences in Caenorhabditis elegans. PLoS One 8: e54971. https://doi.org/10.1371/journal.pone.0054971

Pujol, N., P. Torregrossa, J. J. Ewbank, and J. F. Brunet, 2000 The homeodomain protein CePHOX2/CEH-17 controls antero-posterior axonal growth in C. elegans. Development 127: 3361–3371.

Raizen, D., B. M. Song, N. Trojanowski, and Y. J. You, 2012 Methods for measuring pharyngeal behaviors, (December 18, 2012), *WormBook*, ed. The *C. elegans* Research Community, WormBook, doi/10.1895/wormbook.1.154.1, http://www.wormbook.org.https://doi.org/10.1895/wormbook.1.154.1

Redemann, S., S. Schloissnig, S. Ernst, A. Pozniakowsky, S. Ayloo *et al.*, 2011 Codon adaptation-based control of protein expression in C. elegans. Nat. Methods 8: 250–252. https://doi.org/10.1038/nmeth.1565

Renn, S. C., J. H. Park, M. Rosbash, J. C. Hall, and P. H. Taghert, 1999 A pdf neuropeptide gene mutation and ablation of PDF neurons each cause severe abnormalities of behavioral circadian rhythms in Drosophila. Cell 99: 791–802. https://doi.org/10.1016/S0092-8674(00)81676-1

Ryu, M. H., I. H. Kang, M. D. Nelson, T. M. Jensen, A. I. Lyuksyutova *et al.*, 2014 Engineering adenylate cyclases regulated by near-infrared window light. Proc. Natl. Acad. Sci. USA 111: 10167–10172. https://doi.org/10.1073/pnas.1324301111

Salkoff, L., A. Butler, G. Fawcett, M. Kunkel, C. McArdle *et al.*, 2001 Evolution tunes the excitability of individual neurons. Neuroscience 103: 853–859. https://doi.org/10.1016/S0306-4522(01)00079-3

Schneider, C. A., W. S. Rasband, and K. W. Eliceiri, 2012 NIH Image to ImageJ: 25 years of image analysis. Nat. Methods 9: 671–675. https://doi.org/10.1038/nmeth.2089

Shafer, O. T., D. J. Kim, R. Dunbar-Yaffe, V. O. Nikolaev, M. J. Lohse *et al.*, 2008 Widespread receptivity to neuropeptide PDF throughout the neuronal circadian clock network of Drosophila revealed by real-time cyclic AMP imaging. Neuron 58: 223–237. https://doi.org/10.1016/j.neuron.2008.02.018

Shidara, H., K. Hotta, and K. Oka, 2017 Compartmentalized cGMP responses of olfactory sensory neurons in Caenorhabditis elegans. J. Neurosci. 37: 3753–3763. https://doi.org/10.1523/JNEUROSCI.2628-16.2017

Singh, K., J. Y. Ju, M. B. Walsh, M. A. DiIorio, and A. C. Hart, 2014 Deep conservation of genes required for both Drosphila melanogaster and Caenorhabditis elegans sleep includes a role for dopaminergic signaling. Sleep (Basel) 37: 1439–1451. https://doi.org/10.5665/sleep.3990

Spieth, J., G. Brooke, S. Kuersten, K. Lea, and T. Blumenthal, 1993 Operons in C. elegans: polycistronic mRNA precursors are processed by trans-splicing of SL2 to downstream coding regions. Cell 73: 521–532. https://doi.org/10.1016/0092-8674(93)90139-H

Stinchcomb, D. T., J. E. Shaw, S. H. Carr, and D. Hirsh, 1985 Extrachromosomal DNA transformation of Caenorhabditis elegans. Mol. Cell. Biol. 5: 3484–3496. https://doi.org/10.1128/MCB.5.12.3484

Trojanowski, N. F., and D. M. Raizen, 2016 Call it worm sleep. Trends Neurosci. 39: 54–62. https://doi.org/10.1016/j.tins.2015.12.005

Trojanowski, N. F., M. D. Nelson, S. W. Flavell, C. Fang-Yen, and D. M. Raizen, 2015 Distinct mechanisms underlie quiescence during two Caenorhabditis elegans sleep-like states. J. Neurosci. 35: 14571–14584. https://doi.org/10.1523/JNEUROSCI.1369-15.2015

Trojanowski, N. F., D. M. Raizen, and C. Fang-Yen, 2016 Pharyngeal pumping in Caenorhabditis elegans depends on tonic and phasic signaling from the nervous system. Sci. Rep. 6: 22940. https://doi.org/10.1038/srep22940

Weissenberger, S., C. Schultheis, J. F. Liewald, K. Erbguth, G. Nagel *et al.*, 2011 PACalpha–an optogenetic tool for in vivo manipulation of cellular cAMP levels, neurotransmitter release, and behavior in Caenorhabditis elegans. J. Neurochem. 116: 616–625. https://doi.org/10.1111/j.1471-4159.2010.07148.x

White, J. G., E. Southgate, J. N. Thomson, and S. Brenner, 1986 The structure of the nervous system of the nematode Caenorhabditis elegans. Philos. Trans. R. Soc. Lond. B Biol. Sci. 314: 1–340. https://doi.org/10.1098/rstb.1986.0056

Zhu, Y., Y. Miwa, A. Yamanaka, T. Yada, M. Shibahara *et al.*, 2003 Orexin receptor type-1 couples exclusively to pertussis toxin-insensitive G-proteins, while orexin receptor type-2 couples to both pertussis toxin-sensitive and -insensitive G-proteins. J. Pharmacol. Sci. 92: 259–266. https://doi.org/10.1254/jphs.92.259

Communicating editor: H. Bülow